ACS Sustainable Chemistry & Engineering

Research Article

pubs.acs.org/journal/ascecg

Simultaneous Reinforcement and Toughening of Carbon Nanotube/Cellulose Conductive Nanocomposite Films by Interfacial Hydrogen Bonding

Hua-Dong Huang, Chun-Yan Liu, Liang-Qing Zhang, Gan-Ji Zhong,* and Zhong-Ming Li*

State Key Laboratory of Polymer Materials Engineering, College of Polymer Science and Engineering, Sichuan University, No. 24 South Section 1, Yihuan Road, Chengdu, 610065 Sichuan, People's Republic of China

ABSTRACT: Carbon nanotube (CNT)/cellulose nanocomposite films were prepared by a featured processing method, i.e., solution dispersion, slow gelation and hot-press drying, where an environmentally benign processing solvent (sodium hydroxide/urea aqueous solution) was used. The scanning electron microscopy and transmission electron microscopy demonstrated uniform CNT dispersion in the cellulose. The slow gelation and hot-press drying could effectively reduce the free volume and force the cellulose chains and CNTs to contact as close as possible, thus forming the strong interfacial hydrogen bonding between the residual oxygen-containing functional groups on the CNT surfaces and the hydroxyl groups in the cellulose chains, as confirmed by X-ray photoelectron spectroscopy and Fourier transformation infrared spectroscopy results. As a result, with a CNT loading of 5 wt %, the tensile strength and Young's modulus of the cellulose nanocomposite films were increased by 55% and 21% relative to neat cellulose film. More interestingly, the tensile toughness reached 5.8 MJ/m^3, about 346% higher than that of neat cellulose film. This simultaneous reinforcement and toughening of cellulose by only incorporating the pristine CNTs has been rarely reported. The reason could be explained in the terms of the fortified interfacial hydrogen bonding, which not only facilitated the stress transfer in the interfacial region but also reduced the density of hydrogen bonding network in the intra- and intermolecular chains of cellulose so as to enhance the plastic deformation of the cellulose nanocomposite films significantly. In addition, a good conductivity of 7.2 S·m^{-1} was achieved with a percolation threshold of as low as 0.71 vol %. The strategy proposed here is simple, low cost, efficient and "green", exhibiting great potential for fabricating high-performance and multifunctional CNT/cellulose nanocomposite films used in the realms of antistatic packages, electromagnetic shielding, electrodes, sensors and electric smart brands.

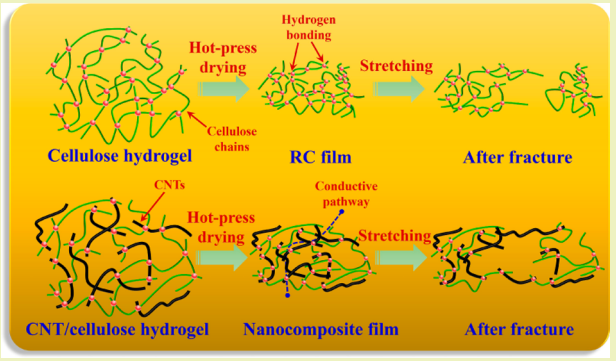

KEYWORDS: *Cellulose, carbon nanotubes, tensile toughness, hydrogen bonding, hot-press drying*

INTRODUCTION

Rapidly growing awareness of environmental pollution and the energy crisis have shifted the focus from traditional petrochemical-based polymeric materials to more environmentally friendly alternatives.[1,2] As such, cellulose, the oldest, most abundant and almost inexhaustible natural biomass resource, has received intensely increasing interest in fundamental research and applications as an ideal green candidate to replace petroleum-based materials in many cases as a result of its many fascinating properties, such as biocompatibility, biodegradability, thermal and chemical stability.[3,4] However, single cellulose film suffers from unbalanced mechanical performances (e.g., low toughness) and limited functionality, which is viewed as a stumbling stone to gravely restrict the development and application of cellulose films. Therefore, it is highly attractive to develop high-performance and multifunctional cellulose films.

Over the past decades, it is well established that the incorporation of nanofillers has been well demonstrated to be an effective strategy to fabricate high-performance and multifunctional hybrid materials.[5−8] Among the nanofillers, carbon nanotubes (CNTs) are one of the most important nanomaterial components. The long-range π-conjugation and large length-diameter ratio endow their unique and superior thermal, mechanical and electrical properties,[9] exhibiting great values or potentials to prepare reinforced and functionalized cellulose nanocomposites. Intuitively, it goes without saying that the addition of CNTs into cellulose films can give them excellent electrical functionality. The electrical cellulose films can have uses in antistatic packaging, electromagnetic shielding, bioelectrode, transistor, sensor and electric smart brands.[10−13] Unfortunately, the enhancement on the conductivity of cellulose nanocomposite films frequently comes at the expense of their mechanical strength.[14−17] For instance, Koga et al. reported that transparent, conductive and printable nanocomposite films were prepared by mixing CNTs and 2,2,6,6-tetramethylpiperidine-1-oxyl-oxidized cellulose nanofibrils,

Received: October 30, 2014
Published: January 4, 2015

DOI: 10.1021/sc500681v
ACS Sustainable Chem. Eng. 2015, 3, 317−324

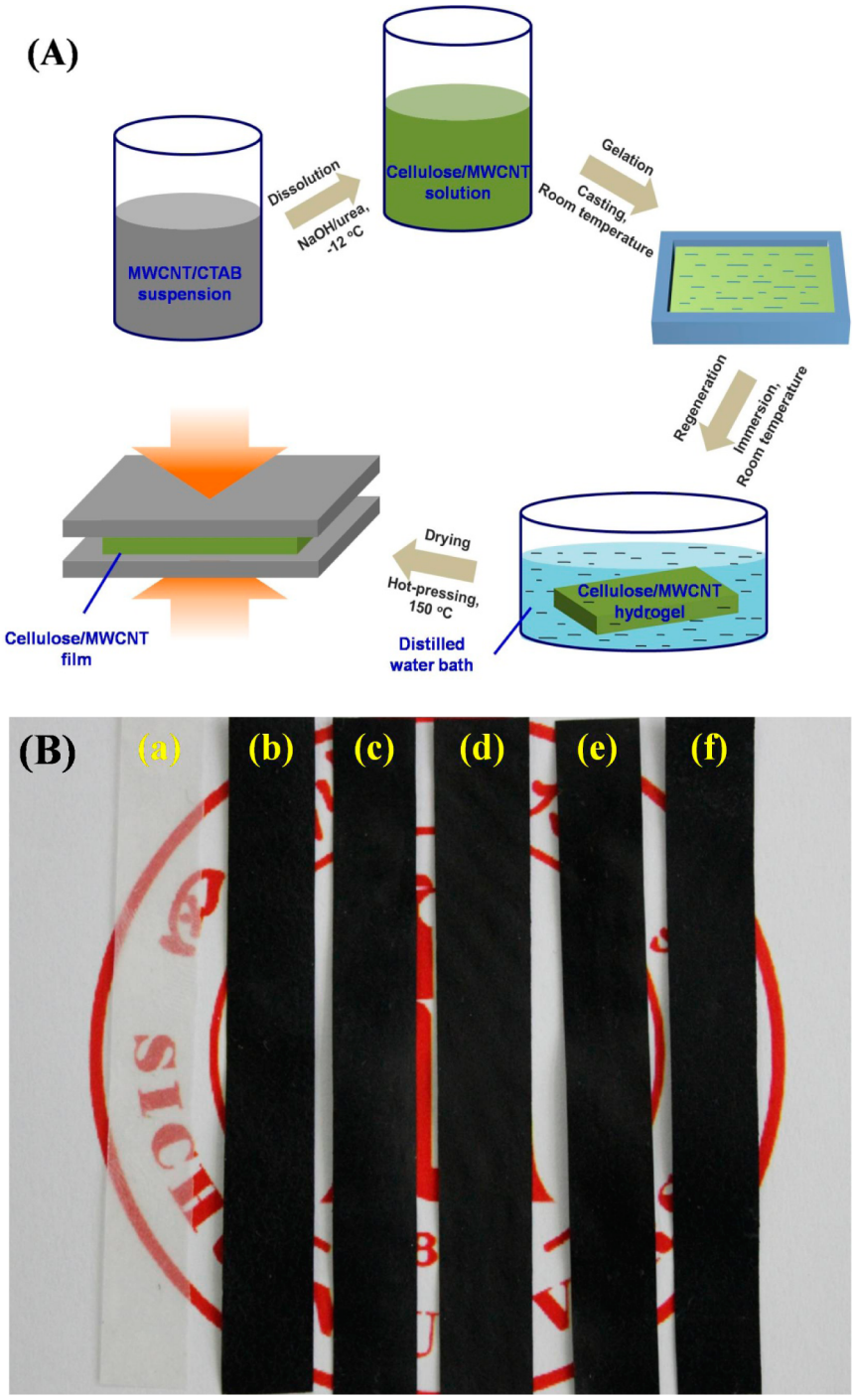

Figure 1. (A) Schematic for the preparation of CNT/cellulose nanocomposite films. (B) Digital photograph of cellulose nanocomposite films with different loadings (0–10 wt %) of CNTs (a–f: RC, MC-1, MC-3, MC-5, MC-8, MC-10).

showing a conductivity as high as ~10 $S \cdot cm^{-1}$. However, the tensile strength of the resultant nanocomposite films tended to deteriorate with increasing CNT content.[16,18] CNTs were also mixed with nanofibrillated cellulose in aqueous suspension and filtered into nanocomposite paper with porous structure. As the content of CNT rose to 16.7 wt %, the tensile strength was gradually reduced from 239 to 66 MPa.[17] On the basis of these studies, the reason for the declined mechanical performances probably stems from the lack of desired interface between cellulose chains and CNTs, giving rise to low effectiveness of load transfer in the interfacial region. In this regard, acid-treatment of CNTs and covalent functionalization of cellulose have been employed to enhance the interfacial interactions, thus, improving tensile strength of cellulose nanocomposite films.[19−21] Yet, the merits of these strategies may be discounted due to the lengthy process and the irreversible long-range π-conjugation damage of CNTs. It thus remains a daunting challenge to achieve the conductive functionalization of cellulose nanocomposite films without compromising its strength and toughness by only taking advantage of pristine CNTs.

DOI: 10.1021/sc500681v
ACS Sustainable Chem. Eng. 2015, 3, 317−324

It is well-known that owing to the supermolecular structure of cellulose with a large proportion of strong inter- and intramolecular hydrogen bonding, the solution process is the main stream to fabricate cellulose-based nanocomposites.[22−25] Sodium hydroxide (NaOH)/urea aqueous solution, developed by Zhang et al.,[24] has been demonstrated to be an effective and promising cellulose solvent owing to its low cost, recyclable, nontoxic and environmentally benign features.[24,26−29] In the current study, aiming at simultaneously functionalizing, reinforcing and toughening cellulose nanocomposite films, a simple preparation process including solution dispersion, slow gelation and hot-press drying was proposed to not only avoid wrinkling of cellulose nanocomposite films but also achieve tight and adequate contacts between multiwalled CNTs and cellulose, resulting in the uniform dispersion of CNTs and strong interfacial adhesion between cellulose chains and CNTs. As a consequence, the tensile strength and Young's modulus of the obtained nanocomposite films were elevated by a large margin at a CNT loading of 5 wt % relative to neat cellulose films. More interestingly, the elongation at break values, especially the tensile toughness, were 163% and 346% higher than that of the neat cellulose films, respectively, which, to the best of our knowledge, had not ever been reported in the literature. In addition, the incorporation of CNTs also endowed cellulose films with a desirable conductivity of 7.2 $S{\cdot}m^{-1}$ and a percolation threshold of as low as 0.71 vol %.

EXPERIMENTAL SECTION

Materials. The cellulose sample (cotton linters, DP 500 ± 50) was supplied by Hubei Jinhuan Ltd. (Xiangfan, China). The multiwalled CNTs with diameters of 20−40 nm and lengths of 10−20 μm were purchased from Chengdu Organic Chemicals Co. Ltd. (Chengdu, China). NaOH (analytical grade), urea (analytical grade) and cetyltrimethylammonium bromide (CTAB, analytical grade) were provided by Kelong Chemical Reagent Factory (Chengdu, China) and used as received.

Preparation of CNT/Cellulose Nanocomposite Films. A certain amount of CNTs was well dispersed in deionized water with the aid of surfactant CTAB by using an ultrasonic cell disruptor for 15 min at a constant output power of 325 W. The weight ratio of surfactant to CNT was adjusted to 0.8:1.0. 7 g of NaOH and 12 g of urea were added to the CNT suspension. The resultant mixture was then precooled to −12.0 °C. A calculated amount of cellulose was added immediately into the mixture with vigorous stirring for 5 min to obtain a homogeneous cellulose solution, in which the concentration of cellulose was kept constant at 2.5 wt %. Thereafter, 20 mL of the resultant CNT/cellulose suspension was cast on a glass plate to give a 10 × 10 cm gel sheet at room temperature, and then immersed in distilled water bath to remove NaOH and urea. The distilled water was replaced regularly with fresh water several times until there were no salts. Finally, the wet films were compressed for 10 min at 150 °C to obtain the CNT/cellulose nanocomposite films. The thickness of these films was about 80 μm and could be controlled by adjusting the volume of CNT/cellulose suspension during the casting process. By changing the amount of CNTs in the aqueous suspension, we fabricated CNT/cellulose nanocomposite films with various CNT loadings: 1, 3, 5, 8 and 10 wt %, which were coded as CM-1, CM-3, CM-5, CM-8 and CM-10, respectively. For comparison, the cellulose film without CNTs was prepared according to the same procedures and coded as RC.

Dispersion Morphology Observation of CNTs. To observe the microstructure of cellulose nanocomposite films, the samples were frozen in liquid nitrogen, and then immediately cryo-fractured. Field-emission scanning electron microscopy (SEM, Inspect F, FEI, Finland) was utilized to image the morphology of cryo-fractured surface, which was sputter-coated with gold before observations, and the accelerated voltage was held at 5 kV. A thin cross section of cellulose nanocomposite film was further imaged via transmission electron microscopy (TEM, FEI Tecnai F20) at an acceleration voltage of 200 kV. The specimen for TEM was prepared by embedding a piece of cellulose nanocomposite film at a CNT loading of 5 wt % in epoxy and a thin cross section was obtained using a microtome equipped with a diamond knife.

Measurement of Interfacial Hydrogen Bonding between CNTs and Cellulose Chains. X-ray photoelectron spectroscopy (XPS) measurements were performed with an XSAM800 (Kratos Company, UK) using Al Kα radiation ($h\nu$ = 1486.6 eV); XPSpeak41 software was used to perform curve fittings. Moreover, Fourier-transform infrared (FTIR) spectra were collected on a Nicolet 6700 FTIR spectrometer with the resolution of 2 cm^{-1} in attenuated total-reflectance mode, in which the obtained spectra had already been subtracted from the background spectra.

Mechanical Testing. According to ASTM standard D638, the mechanical performances of cellulose nanocomposite films were determined on a universal tensile instrument (Model 5576, Instron Instrument, USA) with a span length of 20 mm at a testing speed of 1.0 mm/min. Before testing, the cellulose nanocomposite films were tailored into rectangular strips with the same width of about 10 mm, and the thickness was separately measured for each sample. On the basis of stress−strain curve, the tensile toughness was obtained by integrating the area surrounded by the stress−strain curves.[30,31] The average values and standard deviations of all the mechanical performances (e.g., tensile strength, Young's modulus, elongation at break and tensile toughness) were evaluated by at least five specimens.

Electrical Conductivity Measurement. For electrical conductivity measurements, copper wire nets were stuck to the surface of each sample with silver paste to ensure good contact between sample surfaces with the electrodes. Volume electrical conductivities higher than 10^{-6} $S{\cdot}m^{-1}$ were measured using a Keithley 4200SCS apparatus; volume electrical conductivities below 10^{-6} $S{\cdot}m^{-1}$ were measured using a ZC-36 high-resistance meter. The mean values of at least five measurements for every set of film were calculated.

RESULTS AND DISCUSSION

Microstructure of CNT/Cellulose Nanocomposite Films. Figure 1A schematically illustrates the preparation of CNT/cellulose nanocomposite films, including solution dispersion, slow gelation and hot-press drying. Initially, CNTs were uniformly dispersed in NaOH/urea aqueous solution with the assistance of surfactants. Then cellulose chains turned to be water-soluble as a result of the spontaneously assembled "overcoat" structure, composed of sodium ions, water and urea molecules,[24,26] thus leading to the sufficient contact between cellulose and CNTs at the molecular level. Subsequently, the stable physical cross-linking cellulose networks were gradually formed after a 12 h gelation process at room temperature. Finally, in an attempt to avoid wrinkling, the cellulose nanocomposite hydrogel was rapidly dewatered using hot-press drying to form the resultant CNT/cellulose nanocomposite films. As shown in Figure 1B, the RC film is flexible and semitransparent, and its surface is fairly smooth and uniform, which suggests the superior dissolving capacity of the precooled NaOH/urea aqueous solution to cellulose. During the hot-press drying process, cellulose chains realign in the form of antiparallel chains to form stable cellulose-II crystallites.[28,29,32] The flash evaporation of water in the cellulose nanocomposite hydrogel leads to the small sized cellulose crystallites, thus, making the RC film semitransparent. For the cellulose nanocomposite films, their flexibility is still fairly good and the quality of surface is equal to that of the RC film. The addition of CNTs would not deteriorate the solubility of cellulose in NaOH/urea aqueous solution.

DOI: 10.1021/sc500681v
ACS Sustainable Chem. Eng. 2015, 3, 317−324

To further characterize the dispersion of CNTs in the cellulose matrix, the cryo-fractured surfaces of cellulose nanocomposite films were observed using SEM (Figure 2). It

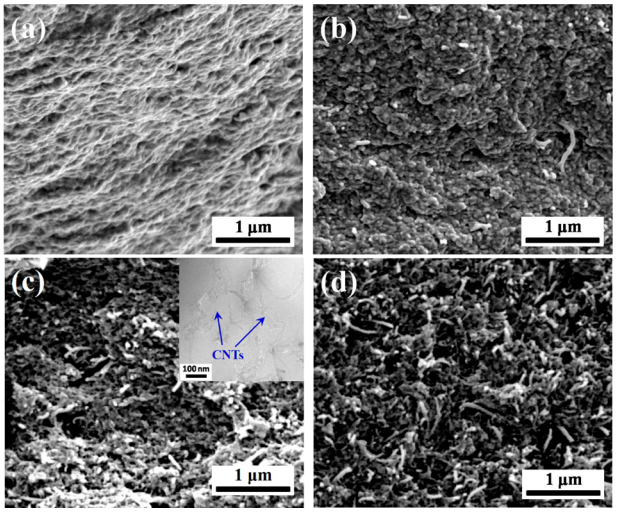

Figure 2. SEM micrographs of the cryo-fractured surface of (a) RC, (b) CM-1, (c) CM-5 and (d) CM-10. The inset in panel c is the TEM image of CM-5.

can be seen that the cryo-fractured surface of the RC film (Figure 2a) displays desirable homogeneity and high compactness, which is quite different from the structure of cellulose films prepared by rapid coagulation with 5 wt % H_2SO_4 solution and air drying at ambient temperature, where porous structure was left after the water volatilization.[33,34] Therefore, the slow gelation and hot-press drying could be introduced as a convenient method to not only shorten the drying time but also force the cellulose phase in the hydrogel to accumulate as close as possible, effectively facilitating the elimination of the voids. In the cellulose nanocomposite films, CNTs are indicated by the bright regions in the SEM images and hollow tubes in the TEM inset image (Figure 2b–d). As the CNT concentration is below 5 wt %, the fibrous structure of CNTs is clearly observed and uniformly dispersed in cellulose matrix without visible aggregates. Even though the CNT concentration rises to 10 wt %, CNTs still remain good dispersion without any traces of CNT aggregates (Figure 2d). The reason for good CNT dispersion is probably attributed to the adequate interfacial interactions between CNTs and cellulose matrix originated from hydrogen bonding, which will be further demonstrated by XPS and FTIR measurements below.

Interfacial Interactions between CNTs and Cellulose Chains. Figure 3a displays the deconvolution of the XPS O 1s peaks of the CNTs, which clearly confirms the presence of some carboxylic and hydroxyl functions onto the CNT surfaces, exhibiting characteristic binding energy at 533.2 and 532.0 eV, respectively.[35] These oxygen-containing functional groups provide the possibility of hydrogen bonding formed between CNTs and cellulose chains. The consistent conclusion can be further verified by FTIR results, as shown in Figure 3b. It is well accepted that the −OH stretching band at the range of 3650–3000 cm^{-1} is sensitive to hydrogen bonding and can be forced to shift to a lower wavenumber.[36,37] It is clearly seen from Figure 3b that the −OH stretching vibration band at around 3325 cm^{-1} in the RC film substantially shifts to a lower wavenumber (3307 cm^{-1}) in CM-1 at a CNT loading of 1 wt

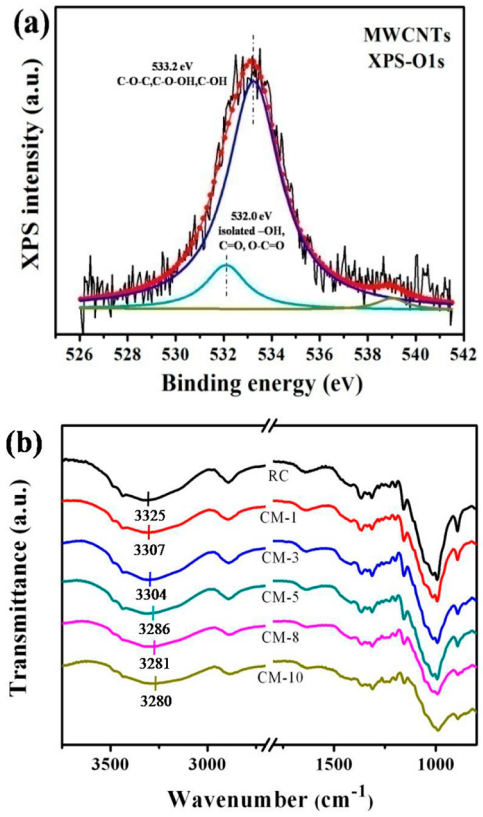

Figure 3. (a) Deconvolution of the XPS O 1s peaks of the CNTs; (b) FTIR spectra of regenerated cellulose and CNT/cellulose nanocomposite films. For clarity, a featureless region is omitted in the range of 2700–1800 cm^{-1}.

% ; when the concentration of CNTs rises to 10 wt %, the −OH stretching vibration of the cellulose in CM-10 further shifts to the lower wavenumber (3280 cm^{-1}). These results can be ascribed to the hydrogen bonding between the residual hydroxyls on the CNT surface and the hydroxyl groups in the cellulose chains. Such strong interfacial interactions are very favorable for the good dispersion of CNTs in the cellulose/NaOH/urea solution, and also the suppression of CNT aggregation during slow gelation and hot-press drying process. As a result, the performances of the final nanocomposite films could be effectively optimized, as shown in next section.

Mechanical Properties of CNT/Cellulose Nanocomposite Films. The typical stress–strain curves of RC and its CNT nanocomposite films are shown in Figure 4. Owing to the rigid characteristic of the cellulose chains, all of the cellulose films fracture in a little brittle manner with limited elongation at break and no distinct yielding or strain hardening.[29,38–40] The addition of CNTs into the cellulose matrix has a significant influence on the tensile deformation behavior. Most attractively, the tensile strength and elongation at break of the nanocomposites apparently exhibit an obvious increase trend simultaneously. The detailed data about mechanical performances are summarized in Figure 5. As shown in Figure 5a,b, the RC film exhibits minimum tensile strength and Young's modulus, i.e., 50.1 MPa and 3.8 GPa, respectively. These values are distinctly different from that reported in the literature, probably depending on the raw materials (e.g., source area, degree of polymerization, and crystallinity), preparation process, solvent and drying method.[38–40] The addition of only

DOI: 10.1021/sc500681v
ACS Sustainable Chem. Eng. 2015, 3, 317–324

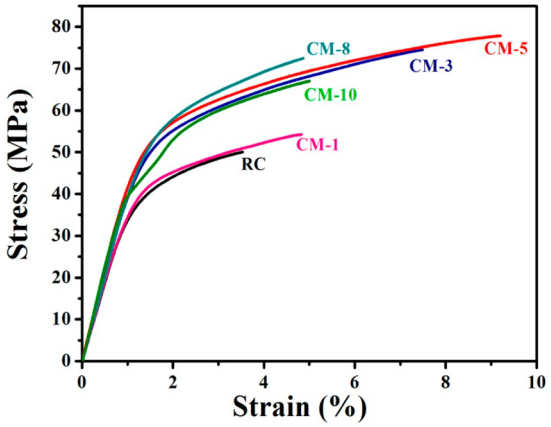

Figure 4. Typical stress–strain curves of RC and CNT/cellulose nanocomposite films as a function of CNT loadings.

1 wt % of CNTs leads to a limited enhancement on the tensile strength and Young's modulus of the cellulose nanocomposite film. Nevertheless, as the CNT concentration rises to 5 wt %, the maximum improvement is seen and the tensile strength and Young's modulus values reach 77.8 MPa and 4.6 GPa, respectively, corresponding to the increases of 55% and 21% relative to the RC films. With further increasing CNT loadings, the tensile strength of the cellulose nanocomposite films is still superior to that of RC films with a slight drop and the Young's modulus is kept constant at 4.6 GPa. This phenomenon manifests that the reinforcement effect of CNTs has a close relationship with the dispersion state of CNTs in the cellulose matrix. At a low content of CNTs (below 5 wt %), the CNTs could be evenly dispersed throughout the entire cellulose matrix (Figure 2b-c). The strong interfacial hydrogen bonding as demonstrated by XPS and FTIR results (Figure 3), is the dominant factor facilitating the stress transfer in the interfacial region, consequently improving the tensile strength and Young's modulus by a large margin. As the content of CNTs is beyond 5 wt %, CNTs are inclined to aggregate due to the strong van der Waals force and their long aspect ratio (Figure 2d). The aggregations disrupt the homogeneity of films and generate the defects in the interfacial region, weakening the enhancement efficiency of CNTs on the mechanical properties of the cellulose nanocomposite films.

The elongation at break and the tensile toughness of RC and its CNT nanocomposite films are illustrated in Figure 5c,d. The elongation at break and the tensile toughness of RC sample are just 3.5% and 1.3 MJ/m^3, respectively. When only 1 wt % CNTs is added, the elongation at break is increased by about 37%, from 3.5 to 4.8%, and the tensile toughness reached 2.0 MJ/m^3 with a 54% increase. More significantly, the elongation at break and tensile toughness of the nanocomposite film with the CNT loading of 5 wt % respectively rises to 9.2% and 5.8 MJ/m^3, which is severally improved by 163% and 346% compared to the RC films. Such simultaneous reinforcement and toughening of cellulose nanocomposite films by only using the pristine CNTs has been rarely reported in the literature. As the content of CNTs is beyond 5 wt %, the unavoidable aggregations of CNTs cause the defects in the interfacial region and significantly reduce the elongation at break and tensile toughness. However, they are still above that of the RC films.

To further reveal the effect of hot-press drying on the improved mechanical properties, the cellulose nanocomposite with CNTs loading of 5 wt % was also fabricated by air drying

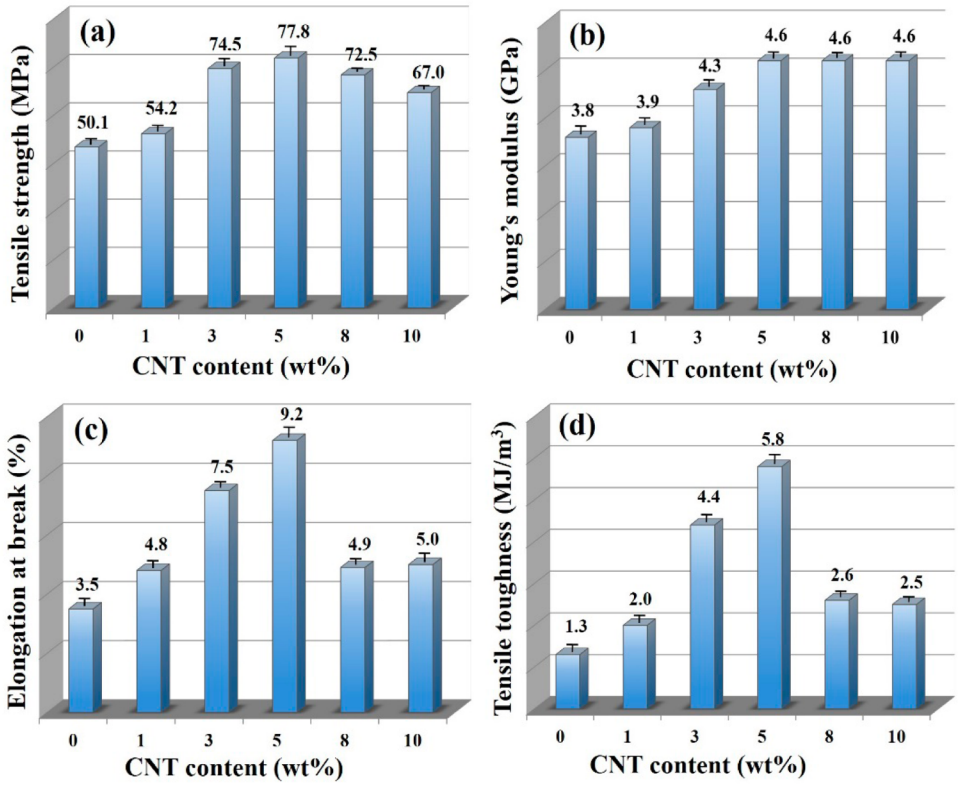

Figure 5. Tensile strength (a), Young's modulus (b), elongation at break (c) and tensile toughness (d) of RC and CNT/cellulose nanocomposite films from Figure 4.

DOI: 10.1021/sc500681v
ACS Sustainable Chem. Eng. 2015, 3, 317–324

for comparison. Its typical stress−strain curve is presented in the inset of Figure 6, exhibiting the tensile strength as low as

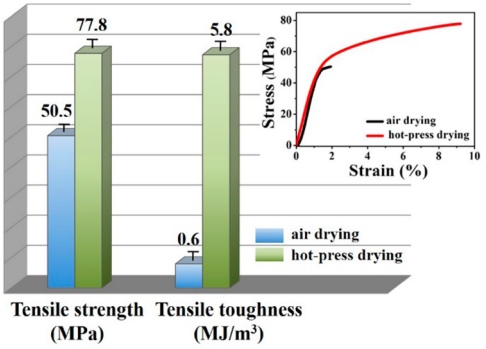

Figure 6. Tensile strength and tensile toughness of CM-5 prepared by air drying and hot-press drying. The inset shows the typical tensile stress−strain curves.

50.5 MPa, much lower than that of the counterpart sample dried by hot pressing at 150 °C. The SEM images of its fractured surfaces (Figure 7a,b) show that some CNTs are

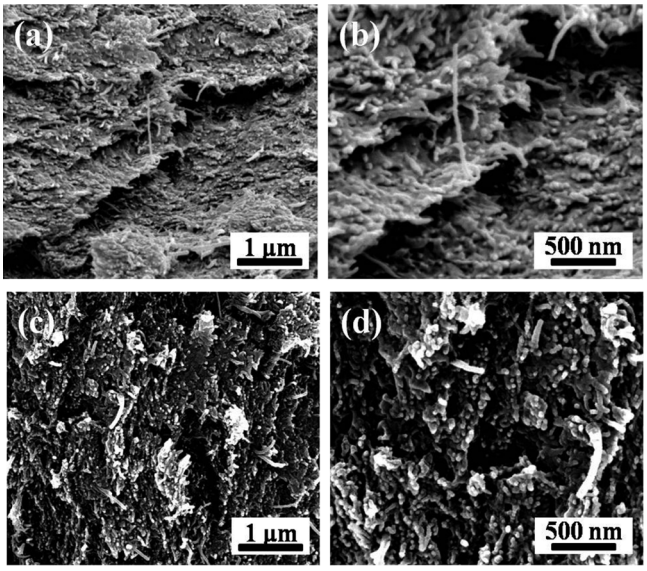

Figure 7. SEM images of the tensile fracture surface of CM-5 prepared by air drying (a,b) and hot-press drying (c,d).

completely pulled-out from the cellulose matrix and voids form in the air-dried cellulose nanocomposite films. In contrast, the fractured morphology of CM-5 prepared by hot-press drying (Figure 7c,d) depicts that the CNTs contact with cellulose more closely so as to form hydrogen bonding more easily. Such strengthened interfacial adhesion is favorable for the stress transfer from the weak cellulose component to carbon nanotubes. As a result, the reinforcement effect of CNTs in our work is more significant. As for the tensile toughness, the air-dried cellulose nanocomposite film is only 0.6 MJ/m^3 due to its inferior interface, further confirming the positive effect of the hot-press drying on toughness.

Electrical Conductivity of CNT/Cellulose Nanocomposite Films. Figure 8 shows the electrical conductivity of CNT/cellulose nanocomposite films as a function of CNT loadings. As only 1 wt % CNTs is added, a typical percolation behavior is

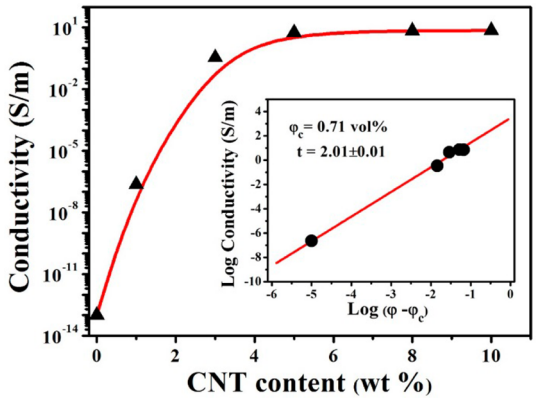

Figure 8. Electrical conductivity as a function of CNT loadings for CNT/cellulose nanocomposite films. The inset shows a log−log plot of the conductivity as a function of $\varphi - \varphi_c$ with an exponent t = 2.01 and a critical volume content φ_c = 0.71 vol %.

clearly observed, displaying a relatively low electrical conductivity of ~10^{-7} S·m^{-1}, but still 6 orders of magnitude higher than that of the RC film. As the CNT loading increases, the well established conductive network of CNTs contributes to higher electrical conductivities. For example, the electrical conductivity rises to 5.6 S·m^{-1} at a CNT loading of 5 wt %. While the CNT loading further increases to 10 wt %, the cellulose nanocomposite film basically achieves a saturated electrical conductivity of 7.2 S·m^{-1}. According to statistical percolation theory, the electrical conductivity is further rationalized in terms of a modified classical percolation theory $\sigma = \sigma_0(\varphi - \varphi_c)^t$, where σ represents the electrical conductivity, σ_0 is the conductivity of filler used, φ is the volume content of CNTs, φ_c is the percolation threshold and t is the critical exponent that describes the mechanism of the conductive network.[41] The inset in Figure 8 shows a plot of log σ versus log($\varphi - \varphi_c$), being indicative of a percolation threshold of approximately 0.71 vol %. This value is very attractive compared with other CNT/cellulose systems,[14,16,17,42] showing an excellent potential for the preparation of antistatic cellulose nanocomposite films at low cost. For a single percolation system, the critical exponent t follows a power-law dependence of approximately 1.6−2.0 in a three-dimensional system, and 1.0−1.3 in a two-dimensional system.[43] Herein, the t value is estimated to be about 2.01, indeed representing a three-dimensional conductive system. This result is in good agreement with the 3D distribution of the CNTs in the nanocomposites as shown in Figure 2.

Mechanism for the Simultaneous Reinforcement and Toughening of Conductive CNT/Cellulose Nanocomposite Films. The above results depicted the panorama of simultaneously reinforced and toughened CNT/cellulose nanocomposite films prepared by solution dispersion, slow-gelation and hot-press drying. In that case, solution blending guaranteed the good dispersion of CNTs in the cellulose matrix. Slow gelation and hot-press drying could effectively reduce the free volume and force the cellulose chains and CNTs to contact as close as possible, thus suppressing the voids in the interfacial region and forming the strong interfacial adhesion. Figure 9 schematically illustrates the structural evolution of RC and its CNT nanocomposite films upon hot-press drying and tensile testing. In the RC film (Figure 9a), the porous cellulose hydrogel is transformed into dense cellulose film by hot-press drying. Nevertheless, owing to the large

DOI: 10.1021/sc500681v
ACS Sustainable Chem. Eng. 2015, 3, 317−324

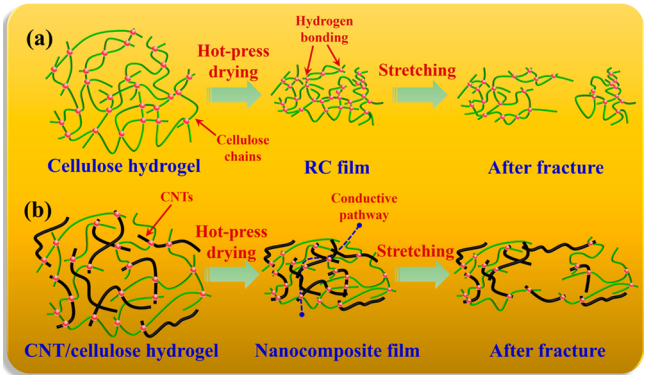

Figure 9. Schematic mechanism for the structural evolution of RC (a) and its CNT nancomposite (b) films upon hot-press drying and tensile testing.

amount of inter- and intramolecular hydrogen bonding, cellulose chains can hardly extend, exhibiting the poor ductility and toughness. On the contrary, in the cellulose nanocomposite films (Figure 9b), the incorporation of CNTs can reduce the density of hydrogen bonding network in the intra- and intermolecular chains of cellulose to some extent and the CNTs bind slightly with their local surrounding. As a result, the plastic deformation of CNT/cellulose nanocomposite films is dramatically enhanced,[44] giving rise to the improved ductility and tensile toughness. Simultaneously, the fortified interfacial interactions ensure the effectiveness of stress transfer in the interfacial region and the tensile strength is elevated by a large margin. Thus, the preparation technique presented here including solution dispersion, slow gelation and hot-press drying is expected to be an ideal choice for solving the dilemma of strength and toughness normally existing in the CNT-reinforced cellulose nanocomposite films.[16,17,45] As for electrical conductivity, the hydrogen bonding is favorable for the good dispersion of CNTs. The hot-press drying densifies the cellulose nanocomposite films and makes the overlap of CNTs take place more easily (Figure 9b), consequently achieving well-established CNT conductive pathways and a desirable conductivity. These results demonstrate that our strong, tough, and conductive cellulose nanocomposite films might have various potential applications such as antistatic packages, electronic devices, biosensors and electric smart brands, etc.

CONCLUSIONS

Nanocomposite films of cellulose and CNTs were successfully prepared using NaOH/urea aqueous solution as the solvent. This was a simple, low cost and "green" pathway to prepare nanocomposite film with both superior mechanical properties and desirable electrical conductivity due to formation of intermolecular hydrogen bonding between CNTs and cellulose chains, as demonstrated by XPS and FTIR. SEM and TEM observations demonstrated that the CNTs were uniformly dispersed in the cellulose matrix. As a result, the obtained cellulose nanocomposite films exhibited significantly improved mechanical strength without sacrificing their toughness. For instance, the tensile strength and tensile toughness of CM-5 film were remarkably enhanced by 55% and 346% compared to the RC film, respectively. Furthermore, this cellulose nanocomposite film possessed a relatively high electrical conductivity (~7.2 $S \cdot m^{-1}$).

AUTHOR INFORMATION

Corresponding Authors

*Tel.: +86-28-8540-6866. Fax: +86-28-8540-6866. E-mail: ganji.zhong@scu.edu.cn (G.-J.Z.).

*Tel.: +86-28-8540-6866. Fax: +86-28-8540-6866. E-mail: zmli@scu.edu.cn (Z.-M.L.).

Notes

The authors declare no competing financial interest.

ACKNOWLEDGMENTS

The authors gratefully acknowledge the National Natural Science Foundation of China (Grants No. 51421061 and 51473101), the Innovation Team Program of Science & Technology Department of Sichuan Province (Grant No. 2014TD0002), the Program of Introducing Talents of Discipline to Universities (B13040) and the Doctoral Program of the Ministry of Education of China (Grant No. 20130181130012 and 20120181120101).

REFERENCES

(1) Sinha Ray, S.; Bousmina, M. Biodegradable polymers and their layered silicate nanocomposites: In greening the 21st century materials world. *Prog. Mater. Sci.* **2005**, *50*, 962−1079.

(2) Tian, H.; Tang, Z.; Zhuang, X.; Chen, X.; Jing, X. Biodegradable synthetic polymers: Preparation, functionalization and biomedical application. *Prog. Polym. Sci.* **2012**, *37*, 237−280.

(3) Klemm, D.; Heublein, B.; Fink, H. P.; Bohn, A. Cellulose: Fascinating biopolymer and sustainable raw material. *Angew. Chem., Int. Ed.* **2005**, *44*, 3358−3393.

(4) Tingaut, P.; Zimmermann, T.; Sèbe, G. Cellulose nanocrystals and microfibrillated cellulose as building blocks for the design of hierarchical functional materials. *J. Mater. Chem.* **2012**, *22*, 20105−20111.

(5) Sinha Ray, S.; Okamoto, M. Polymer/layered silicate nanocomposites: A review from preparation to processing. *Prog. Polym. Sci.* **2003**, *28*, 1539−1641.

(6) Spitalsky, Z.; Tasis, D.; Papagelis, K.; Galiotis, C. Carbon nanotube−polymer composites: Chemistry, processing, mechanical and electrical properties. *Prog. Polym. Sci.* **2010**, *35*, 357−401.

(7) Kuilla, T.; Bhadra, S.; Yao, D.; Kim, N. H.; Bose, S.; Lee, J. H. Recent advances in graphene based polymer composites. *Prog. Polym. Sci.* **2010**, *35*, 1350−1375.

(8) Li, B.; Hahm, M. G.; Kim, Y. L.; Jung, H. Y.; Kar, S.; Jung, Y. J. Highly organized two-and three-dimensional single-walled carbon nanotube-polymer hybrid architectures. *ACS Nano* **2011**, *5*, 4826−4834.

(9) Ajayan, P. Nanotubes from carbon. *Chem. Rev.* **1999**, *99*, 1787−1800.

(10) Kim, J. H.; Yun, S.; Ko, H. U.; Kim, J. A flexible paper transistor made with aligned single-walled carbon nanotube bonded cellulose composite. *Curr. Appl. Phys.* **2013**, *13*, 897−901.

(11) Qi, H. S.; Mader, E.; Liu, J. W. Unique water sensors based on carbon nanotube-cellulose composites. *Sens. Actuators, B* **2013**, *185*, 225−230.

(12) Tanaka, T.; Sano, E.; Imai, M.; Akiyama, K. Electrical conductivity of carbon-nanotube/cellulose composite paper. *J. Appl. Phys.* **2010**, *107*, 054307.

(13) Wu, X. E.; Zhao, F.; Varcoe, J. R.; Thumser, A. E.; Avignone-Rossa, C.; Slade, R. C. T. Direct electron transfer of glucose oxidase immobilized in an ionic liquid reconstituted cellulose-carbon nanotube matrix. *Bioelectrochemistry* **2009**, *77*, 64−68.

(14) Hamedi, M. M.; Hajian, A.; Fall, A. B.; Hakansson, K.; Salajkova, M.; Lundell, F.; Wagberg, L.; Berglund, L. A. Highly conducting, strong nanocomposites based on nanocellulose-assisted aqueous dispersions of single-wall carbon nanotubes. *ACS Nano* **2014**, *8*, 2467−2476.

DOI: 10.1021/sc500681v
ACS Sustainable Chem. Eng. 2015, 3, 317−324

(15) Imai, M.; Akiyama, K.; Tanaka, T.; Sano, E. Highly strong and conductive carbon nanotube/cellulose composite paper. *Compos. Sci. Technol.* **2010**, *70*, 1564−1570.
(16) Koga, H.; Saito, T.; Kitaoka, T.; Nogi, M.; Suganuma, K.; Isogai, A. Transparent, conductive, and printable composites consisting of TEMPO-oxidized nanocellulose and carbon nanotube. *Biomacromolecules* **2013**, *14*, 1160−1165.
(17) Salajkova, M.; Valentini, L.; Zhou, Q.; Berglund, L. A. Tough nanopaper structures based on cellulose nanofibers and carbon nanotubes. *Compos. Sci. Technol.* **2013**, *87*, 103−110.
(18) Saito, T.; Nishiyama, Y.; Putaux, J.-L.; Vignon, M.; Isogai, A. Homogeneous suspensions of individualized microfibrils from TEMPO-catalyzed oxidation of native cellulose. *Biomacromolecules* **2006**, *7*, 1687−1691.
(19) Kim, D. H.; Park, S. Y. In-situ preparation of multi-walled carbon nanotube (MWNT)/cellulose nanocomposites and their physical properties. *Fiber Polym.* **2013**, *14*, 566−570.
(20) Yun, S.; Kang, K. S.; Kim, J. Effect of covalent bonds on the mechanical properties of a multi-walled carbon nanotube/cellulose composite. *Polym. Int.* **2010**, *59*, 1071−1076.
(21) Yun, S.; Kim, J. Covalently bonded multi-walled carbon nanotubes-cellulose electro-active paper actuator. *Sens. Actuators, A* **2009**, *154*, 73−78.
(22) Striegel, A. Theory and applications of DMAc/LiCl in the analysis of polysaccharides. *Carbohydr. Polym.* **1997**, *34*, 267−274.
(23) Fink, H.-P.; Weigel, P.; Purz, H.; Ganster, J. Structure formation of regenerated cellulose materials from NMMO-solutions. *Prog. Polym. Sci.* **2001**, *26*, 1473−1524.
(24) Cai, J.; Zhang, L. Rapid dissolution of cellulose in LiOH/urea and NaOH/urea aqueous solutions. *Macromol. Biosci.* **2005**, *5*, 539−548.
(25) Zhu, S.; Wu, Y.; Chen, Q.; Yu, Z.; Wang, C.; Jin, S.; Ding, Y.; Wu, G. Dissolution of cellulose with ionic liquids and its application: A mini-review. *Green Chem.* **2006**, *8*, 325−327.
(26) Cai, J.; Zhang, L. Unique gelation behavior of cellulose in NaOH/urea aqueous solution. *Biomacromolecules* **2006**, *7*, 183−189.
(27) Cai, J.; Zhang, L.; Zhou, J.; Qi, H.; Chen, H.; Kondo, T.; Chen, X.; Chu, B. Multifilament fibers based on dissolution of cellulose in NaOH/urea aqueous solution: Structure and properties. *Adv. Mater.* **2007**, *19*, 821−825.
(28) Liu, C.-Y.; Zhong, G.-J.; Huang, H.-D.; Li, Z.-M. Phase assembly-induced transition of three dimensional nanofibril-to sheet-networks in porous cellulose with tunable properties. *Cellulose* **2014**, *21*, 383−394.
(29) Huang, H.-D.; Liu, C.-Y.; Li, D.; Chen, Y.-H.; Zhong, G.-J.; Li, Z.-M. Ultra-low gas permeability and efficient reinforcement of cellulose nanocomposite films by well-aligned graphene oxide nanosheets. *J. Mater. Chem. A* **2014**, *2*, 15853−15863.
(30) Xu, H.; Zhong, G.-J.; Fu, Q.; Lei, J.; Jiang, W.; Hsiao, B. S.; Li, Z.-M. Formation of shish-kebabs in injection-molded poly (L-lactic acid) by application of an intense flow field. *ACS Appl. Mater. Interfaces* **2012**, *4*, 6774−6784.
(31) Song, P. a.; Xu, Z.; Guo, Q. Bioinspired strategy to reinforce PVA with improved toughness and thermal properties via hydrogen-bond self-assembly. *ACS Macro Lett.* **2013**, *2*, 1100−1104.
(32) Gupta, P.; Uniyal, V.; Naithani, S. Polymorphic transformation of cellulose I to cellulose II by alkali pretreatment and urea as an additive. *Carbohydr. Polym.* **2013**, *94*, 843−849.
(33) Yang, Q.; Qin, X.; Zhang, L. Properties of cellulose films prepared from NaOH/urea/zincate aqueous solution at low temperature. *Cellulose* **2011**, *18*, 681−688.
(34) Li, R.; Zhang, L.; Xu, M. Novel regenerated cellulose films prepared by coagulating with water: Structure and properties. *Carbohydr. Polym.* **2012**, *87*, 95−100.
(35) Datsyuk, V.; Kalyva, M.; Papagelis, K.; Parthenios, J.; Tasis, D.; Siokou, A.; Kallitsis, I.; Galiotis, C. Chemical oxidation of multiwalled carbon nanotubes. *Carbon* **2008**, *46*, 833−840.
(36) Yan, Z.; Chen, S.; Wang, H.; Wang, B.; Jiang, J. Biosynthesis of bacterial cellulose/multi-walled carbon nanotubes in agitated culture. *Carbohydr. Polym.* **2008**, *74*, 659−665.
(37) Huang, H.-D.; Ren, P.-G.; Chen, J.; Zhang, W.-Q.; Ji, X.; Li, Z.-M. High barrier graphene oxide nanosheet/poly(vinyl alcohol) nanocomposite films. *J. Membr. Sci.* **2012**, *409*, 156−163.
(38) Han, D.; Yan, L.; Chen, W.; Li, W.; Bangal, P. Cellulose/graphite oxide composite films with improved mechanical properties over a wide range of temperature. *Carbohydr. Polym.* **2011**, *83*, 966−972.
(39) Kim, C.-J.; Khan, W.; Kim, D.-H.; Cho, K.-S.; Park, S.-Y. Graphene oxide/cellulose composite using NMMO monohydrate. *Carbohydr. Polym.* **2011**, *86*, 903−909.
(40) Zhang, X.; Liu, X.; Zheng, W.; Zhu, J. Regenerated cellulose/graphene nanocomposite films prepared in DMAC/LiCl solution. *Carbohydr. Polym.* **2012**, *88*, 26−30.
(41) Hu, L.; Hecht, D.; Grüner, G. Percolation in transparent and conducting carbon nanotube networks. *Nano Lett.* **2004**, *4*, 2513−2517.
(42) Anderson, R. E.; Guan, J.; Ricard, M.; Dubey, G.; Su, J.; Lopinski, G.; Dorris, G.; Bourne, O.; Simard, B. Multifunctional single-walled carbon nanotube−cellulose composite paper. *J. Mater. Chem.* **2010**, *20*, 2400−2407.
(43) Gao, J.-F.; Li, Z.-M.; Meng, Q.-j.; Yang, Q. CNTs/UHMWPE composites with a two-dimensional conductive network. *Mater. Lett.* **2008**, *62*, 3530−3532.
(44) Wang, M.; Anoshkin, I. V.; Nasibulin, A. G.; Korhonen, J. T.; Seitsonen, J.; Pere, J.; Kauppinen, E. I.; Ras, R. H.; Ikkala, O. Modifying native nanocellulose aerogels with carbon nanotubes for mechanoresponsive conductivity and pressure sensing. *Adv. Mater.* **2013**, *25*, 2428−2432.
(45) Qi, H. S.; Liu, J. W.; Gao, S. L.; Mader, E. Multifunctional films composed of carbon nanotubes and cellulose regenerated from alkaline-urea solution. *J. Mater. Chem. A* **2013**, *1*, 2161−2168.

DOI: 10.1021/sc500681v
ACS Sustainable Chem. Eng. 2015, 3, 317−324